JOURNAL OF APPLIED ELECTROCHEMISTRY **28** (1998) 96–102

Surface modification of Inconel-600 by growth of a hydrous oxide film

D. MARIJAN*, M. VUKOVIĆ

Ruđer Bošković Institute, POB 1016, HR-10000 Zagreb, Croatia

P. PERVAN, M. MILUN

Institute of Physics, POB 304, HR-10000 Zagreb, Croatia

Received 11 November 1996; revised 8 March 1997

In this study, Inconel-600 (Ni–Cr–Fe alloy) was modified by repetitive potential cycling in 1 M NaOH solution. This procedure induced the growth of a hydrous oxide film, following the same mechanism as previously reported for pure nickel in alkaline solution under similar experimental conditions. The electrode, modified by 30 repetitive potential cycles, exhibited about one order of magnitude lower current density in both the active and passive ranges of the anodic polarization curve. Selective dissolution of nickel and iron in acid solution was determined by rotating ring–disc electrode measurements. This process resulted in chromium enrichment as shown by use of X-ray electron spectroscopy. The proposed model for the enhanced stability of the modified electrode agrees with the percolation model of passivity of stainless steels and Fe–Cr alloys.

Keywords: *alloy*, *Inconel-600*, *surface modification*

1. Introduction

The surface modification of noble and some transition metal (Fe, Ni, W, Co) electrodes by electrochemically produced thick hydrous oxide films, usually brought about by continuous potential cycling, has been the subject of numerous investigations [1, 2]. In some cases, when compared with pure metals, the hydrous oxide films exhibited better electrocatalytic properties in chlorine [3] and oxygen [4–6] evolution reactions, although their stability did not match the stability of anhydrous oxide films [7].

In the particular case of iron [8–10] and nickel [11–13], which are the main components of Inconel-600 alloy, Burke *et al.* and Arvia *et al.* described the experimental conditions for the hydrous oxide growth. During the oxide growth the electrochemical processes were characterized by a pair of reversible peaks due to $Fe(OH)_2$/FeOOH and $Ni(OH)_2$/NiOOH transitions. In the case of stainless steel (AISI-302), the hydrous oxide growth was achieved by potential cycling in alkaline solution, evidenced by an increase in voltammetric charge within the same potential range as was obtained with pure iron and nickel [14].

The significance of the electrochemistry of hydrous oxide films in corrosion processes and passive oxide film formation is primarily in the fact that the role of water in these processes is still a controversial issue. In the crystalline model of passivity of iron, it is generally accepted that the passive layer consists of a compact inner (Fe_3O_4) and outer (Fe_2O_3) oxide layers [15], with OH groups and water molecules adsorbed at the oxide surface. This model has recently been supported by the XANEX data of Davenport and Sansone [16]. However, as the literature survey reported by these authors shows, no conclusive agreement on the structure of the passive oxide film on iron has yet been reached.

The second model is based on the findings that water may be incorporated in the iron oxide films [17–19]. This is the so called 'polymeric-hydrated-oxide' model of passivity. This was also applied on a passive oxide film on stainless steel [20] and in this case a significant role of water in its stability was indicated. In the case of multicomponent systems containing Cr, a chromium-like behaviour is expected when its content exceeds 12%. Indeed, it is well known that the enrichment of Cr takes place in the passive layer of Cr-containing alloys and contributes predominantly to the metal's stability [21].

The modification of metal surfaces for the purpose of improving their corrosion resistance has received a great deal of attention [22]. For example, a stainless steel surface modified by square-wave polarization in sulphuric acid exhibited enhanced stability as shown by Mansfeld *et al.* [23]. Lalvani and Zhang investigated the corrosion of carbon steel using periodic voltage modulation [24]. Various rates of corrosion were observed depending on the level of d.c. potential and type of alternating voltage modulation used. A

* Present address: PLIVA d. o. o. Research Institute, B. Filipovicá 25, HR-10000 Zagreb, Croatia.

 0021-891X

hydrous oxide film on stainless steel, produced in an alkaline solution, exhibited enhanced stability in sulphuric acid [14].

In this work, the modification of Inconel-600 has been achieved by repetitive potential cycling in 1 M NaOH solution. The aim of this work is to determine the experimental conditions needed for hydrous oxide growth on Inconel-600 and to what extent such a layer contributes to corrosion properties of this alloy.

2. Experimental details

The working electrode, Inconel-600 (Ni 72%, Cr 15.5%, Fe 8%,Goodfellow, Cambridge) in the form of a wire of 0.1 cm diameter, 0.25 cm^2 area, was fixed to a glass tube using epoxy resin. The surface was polished using emery paper and 0.05 μm alumina powder, degreased by acetone, ethyl alcohol, and washed with quadruply distilled water. After these cleaning steps, the electrode was immediately immersed in the cell and polarized cathodically at −0.6 V vs SCE in 0.5 M H_2SO_4 (Fluka puriss. p.a.) for 5 min. All stated potentials are referred to SCE. A platinum foil was used as a counter electrode. The polishing procedure and cathodic polarization were repeated before each preparation of oxide film.

The second form of the working electrode was a Pine (model AFMT135PTPT) rotating ring–disc electrode (RRDE) with interchangeable disc. The Inconel-600 disc and platinum ring were of 0.2 cm^2 and 0.11 cm^2 area, respectively. The collection efficiency for this electrode system was 0.2 [25]. The RRDE system was driven by a Pine (model AFMSRXE) rotator. The electrode rotated at 2500 revolutions per minute (rpm).

The oxide was grown by repetitive potential cycling in a 1 M NaOH solution (Fluka puriss. p.a.) using an EG&G 273/97 potentiostat/galvanostat. In a comparative experiment, the potentiostatic oxide growth was carried out at 0.5 V in 1 M NaOH.

The XPS measurements were carried out on four Inconel-600 samples of area about 0.65 cm^2 each. Prior to the XPS measurements the four samples were electrochemically and chemically treated in the following way:

Sample 1. One potentiodynamic sweep between −1.2 and 0.5 V in 1M NaOH solution.
Sample 2. Same as sample 1 followed by immersion in 0.5 M H_2SO_4 for 2 min.
Sample 3. 30 cyclic potentiodynamic sweeps between −1.2 and 0.5 V
Sample 4. Same as sample 3 followed by immersion in 0.5 M H_2SO_4 for 2 min.

In all cases the electrodes were withdrawn from a sodium hydroxide solution at 0.5 V, washed, dried in a desiccator under low vacuum conditions, and transferred into the ultrahigh vacuum chamber of the spectrometer. The spectrometer consists of a hemispherical analyser (Vacuum Science Workshop HA 100) and a Mg/Al dual-anode X-ray source. The excitation energy was 1253.6 eV (MgK_α line). The as-received samples showed, as expected, carbon as the main surface component. To reduce surface carbon concentration, all samples were sputtered for 1 min with Ar^+ ions of 300 eV energy. This procedure did not significantly affect the surface concentration of the main components of the alloy (as shown by repetitive sputtering experiments), but significantly reduced the concentration of impurities, with carbon being the most common.

Open-circuit decay curves and anodic potentiodynamic curves were recorded in 0.5 M H_2SO_4 solution. The open-circuit potential curves at a RRDE were measured in 0.1 M $Na_2SO_4 \cdot 10H_2O$ (Kemika, p.a.) adjusted to pH 2.7. The solutions were deaerated using purified nitrogen. All measurements were carried out at room temperature.

3. Results

3.1. *Optimal experimental conditions for hydrous oxide growth*

The cyclic voltammograms of Inconel-600, before and after 30 repetitive potentiodynamic sweeps performed without holding the potential at either positive or negative potential limits in 1 M NaOH solution, are shown in Fig. 1. A small peak shows up at −1.0 V only during the first sweep in the positive direction. A pair of reversible peaks is located between 0.2 V and 0.4 V. An increase in the voltammetric charge, which is used here as a measure of the charge storage capacity of these peaks, is also evident after repetitive cycling. As the accuracy of the charge integration of the anodic peak (Fig. 1) is affected by a broad shoulder between 0.1 V and 0.35 V (particularly in the first cycle), the integration of current below the cathodic peak at 0.3 V is chosen as a measure of the oxide growth. The voltammetric charge of the cathodic peak at 0.3 V does not vary significantly with the lower potential limit (Fig. 2(a)), whereas it is significantly dependent on the upper potential limit (Fig. 2b): it increases while entering the region of oxygen evolution reaction, at 0.4 V.

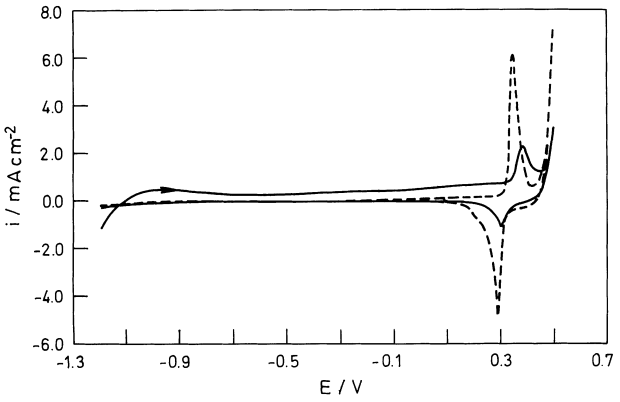

Fig. 1. Cyclic voltammograms at a sweep rate of 50 mV s^{-1} of the Inconel-600 wire electrode in 1 M NaOH. First cycle (full line), after 30 repetitive potentiodynamic sweeps from −1.2 V to 0.5 V at 50 mV s^{-1} (dashed line).

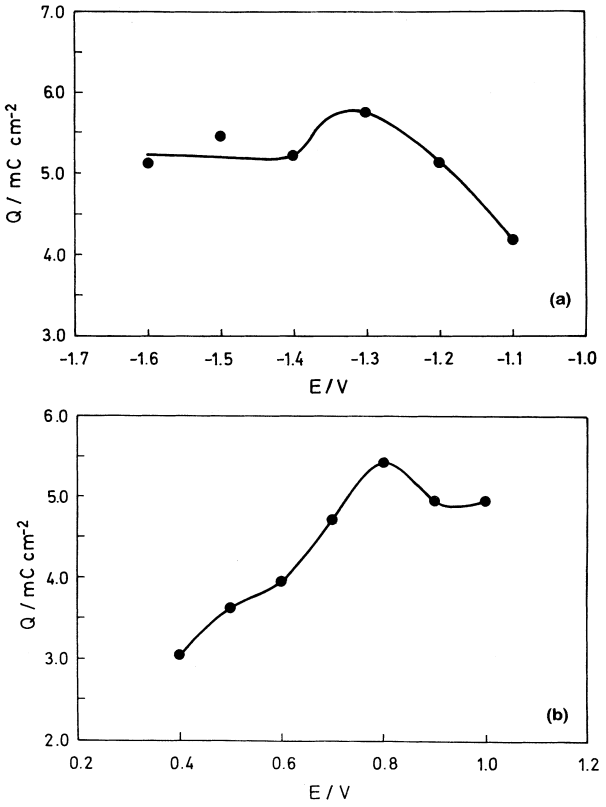

Fig. 2. Charge capacity associated with the cathodic peak at 0.3 V (Fig. 1) as a function of lower limit of potential sweep after 30 cycles at 50 mV s^{-1} in 1 M NaOH. The upper limit was fixed at 0.5 V (a); and charge capacity as a function of the upper limit of potential (b). The lower limit was fixed at −1.2 V. The analytical cyclic voltammogram was recorded at 50 mV s^{-1} between −1.2 V and 0.5 V.

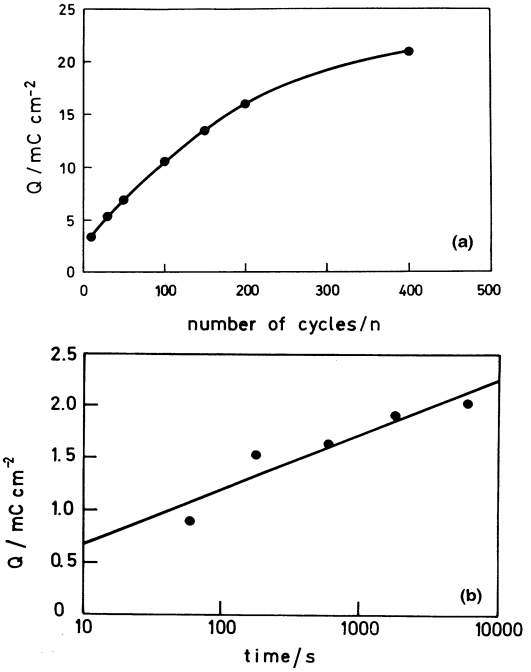

Fig. 3. Charge capacity associated with the cathodic peak at 0.3 V (Fig. 1) as a function of number of cycles. The oxide was grown at 50 mV s^{-1} between −1.3 and 0.5 V in 1 M NaOH (a), and charge capacity as a function of polarization at 0.5 V in 1 M NaOH (b). The analytical cyclic voltammogram was recorded between −1.2 V and 0.5 V at 50 mV s^{-1}.

The voltammetric charge of the cathodic peak at 0.3 V as a function of the number of cycles is presented in Fig. 3(a). After 400 cycles, the charge approaches a plateau of about 20–25 mC cm^{-2}. To compare the repetitive potentiodynamic with potentiostatic oxide growth, the charge as a function of potentiostatic polarization time at 0.5 V is also shown in Fig. 3(b). A direct logarithmic dependence is thus obtained. From the cyclic voltammogram in Fig. 1, it is evident that the oxide formation potential is between 0.3 V and 0.5 V (the main oxidation peak due to $Ni(OH)_2$/NiOOH transition). The sweep rate was 50 mV s^{-1} (i.e., 4 s per cycle in the corresponding potential range). The cumulative time for surface oxidation after 400 cycles was 1600 s. The voltammetric charge associated with the reduction of NiOOH was 20 mC cm^{-2}. After potentiostatic oxidation during 1600 s, the charge of the corresponding nickel peak was 1.6 mC cm^{-2}.

3.2. *Stability of the oxide film*

To monitor the stability of the grown oxide film on Inconel-600 we have used three different techniques: anodic potentiodynamic polarization, the RRDE, and open-circuit potential measurements.

Figure 4 shows the anodic potentiodynamic polarization curves of the untreated Inconel-600 electrode together with the polarization plot of the electrode modified by 30 repetitive potential cycles. Surface modification was carried out in a 1 M NaOH solution, and the stability test in a 0.5 M H_2SO_4 solution. The corrosion potential at about −0.4 V is observed for both electrodes. The most significant result obtained was a decrease of current observed in both the active and passive ranges in the case of the modified electrode. In the transpassive region both curves overlap.

In the stability test, using RRDE measurements, the oxide was grown by 30 repetitive potential cycles on an Inconel-600 disc electrode in 1 M NaOH. After 30 cycles the electrode was withdrawn from the solution at 0.5 V, transferred into another cell with an

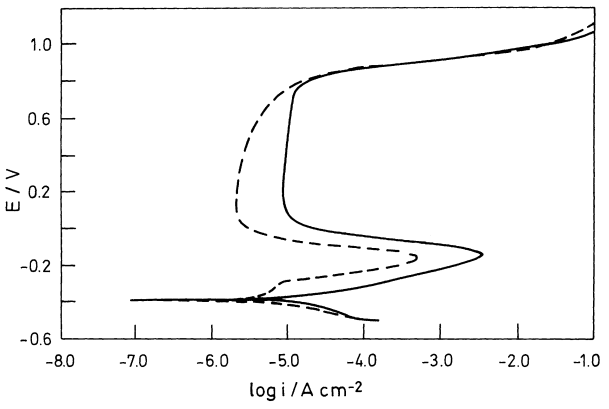

Fig. 4. Anodic polarization curves at 1 mV s^{-1} in 0.5 M H_2SO_4 for untreated Inconel-600 electrode (full line) and for the Inconel-600 electrode subjected to 30 repetitive potentiodynamic sweeps at 50 mV s^{-1} between −1.3 V and 0.5 V in 1 M NaOH (dashed line).

electrolyte of pH 2.7 (0.1 M $Na_2SO_4 \cdot 10H_2O$ + H_2SO_4) and held at open-circuit potential. The platinum ring electrode, on which dissolved species from the disc were detected, was held at 0.6 V. The cyclic voltammogram of a mixture of Fe(II) and Ni(II) salts showed that at this potential, both Fe(II) and Ni(II) species were oxidized to Fe(III) and Ni(III), respectively [26]. The ring current of the electrode treated by 30 repetitive potential cycles, decreased after 10 s to the same value as the current of the untreated electrode, evidencing the instability of the grown oxide layer (Fig. 5).

The third stability test, performed as an open-circuit potential measurement in a 0.5 M H_2SO_4 solution, shows that the most stable surface is the one produced on the potentiodynamically modified electrode (Fig. 6). The open-circuit potential of the untreated electrode was in the active potential range from the very beginning of the experiment. The open-circuit potential of the potentiostatically modified electrode (not shown) differs by less than about 10% from that of the untreated electrode. The most complex E/t behaviour is exhibited by the electrode modified by 30 repetitive potential cycles. At the beginning of the open-circuit potential measurements, the potential was more positive by 0.4 V than that detected on the untreated electrode. The potential was on the positive side for about 10 min before it dropped to a negative value. This sharp decrease of potential was detected at 0.05 V, reaching eventually a value of about −0.2 V.

3.3. *Cyclic voltammetric characterization of the Inconel-600 surface after a stability test*

It was of interest to characterize the state of the surface of the electrode modified by 30 cycles during open-circuit potential measurements. In a separate set of measurements, the electrode with an oxide film grown by 30 repetitive potential cycles in 1 M NaOH was withdrawn from the acidic solution (0.5 M H_2SO_4) after the stability test, and transferred into the cell containing a 1 M NaOH solution. The cyclic

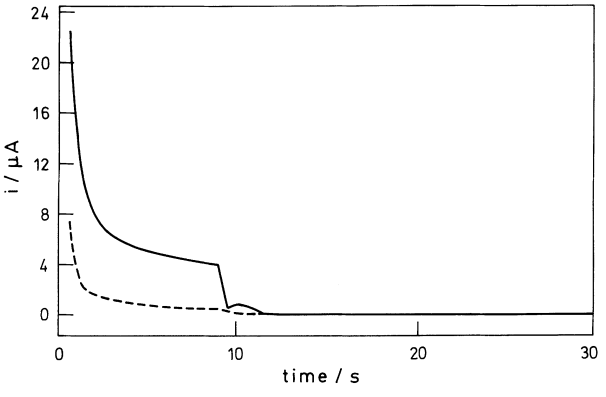

Fig. 5. Ring current–time curves in 0.1 M Na_2SO_4 solution adjusted to pH 2.7 of the untreated Inconel-600 electrode (dashed line); and of the Inconel-600 electrode cycled 30 times between −1.2 V and 0.5 V in 1 M NaOH (full line). Rotation speed 2500 rpm.

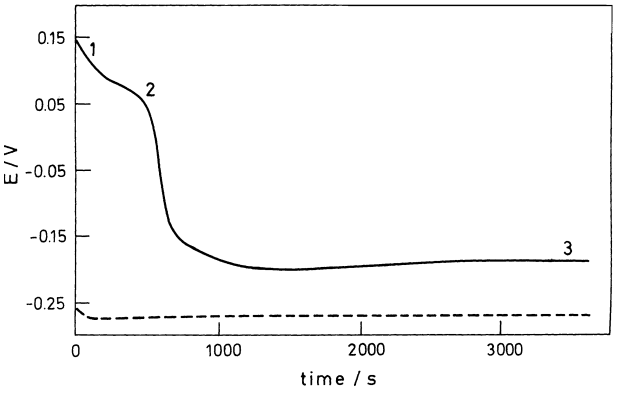

Fig. 6. Open-circuit potential in 0.5 M H_2SO_4 of the untreated Inconel-600 electrode (dashed line) and of the Inconel-600 electrode cycled 30 times between −1.2 V and 0.5 V in 1 M NaOH (full line).

voltammogram (Fig. 7), performed at point 1 in Fig. 6, was taken before the open-circuit potential measurements and, as a matter of fact, is the same as the voltammogram already presented in Fig. 1. It has been repeated here to obtain a better look at the other two voltammograms recorded at points 2 and 3. The most electrochemically inactive surface is at point 2 of the open-circuit potential curve. It is clearly manifested in the shape of the corresponding voltammogram in Fig. 7: the current varies only a little, giving rise to a broad shoulder where the point-1 voltammogram displays a strong peak. At point 3 (i.e., in the active range) the voltammetric charge is increased, and the poorly developed shoulder of the point-2 voltammogram develops into a distinct peak (Fig. 7, full line).

3.4. *XPS characterization of the modified layer*

Although cyclic voltammetry gives an insight into surface electrochemical oxidation/reduction processes of bare and modified electrode surfaces, more direct surface analysis is necessary to determine the surface composition before and after various steps of electrode modification. In this connection, XPS analysis was carried out after 1 and 30 potential cycles in 1 M

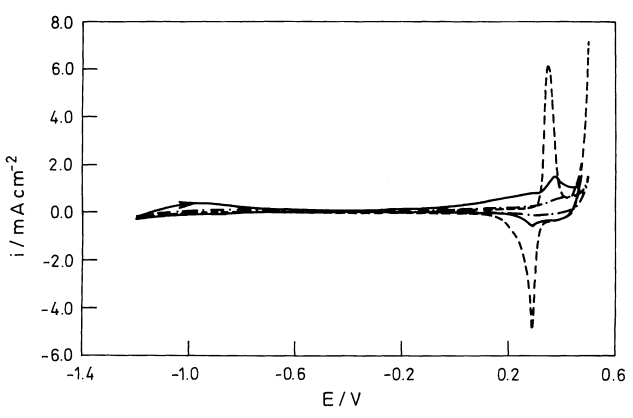

Fig. 7. Cyclic voltammograms at a sweep rate of 50 mV s^{-1} in 1 M NaOH recorded at (– – –) point 1; (— · – · –) point 2, and (——) point 3 of the open-circuit potential curve in Fig. 6.

NaOH solution, followed by a stability test in a 0.5 M H_2SO_4 solution. More precisely, XPS analysis was carried out with the samples taken from the solution at point 1 of the open-circuit potential curve (Fig. 6) and after a 2 min immersion in sulphuric acid (i.e., between points 1 and 2 at the open-circuit potential curve). As can be seen in Table 1, four samples were analysed (see Section 2) to determine the Cr/Ni ratio. The concentration of a constituent was obtained by recording its 2p level and measuring the peak area after the background had been subtracted using the Shirley method. The obtained peak area was then corrected for the corresponding ionization cross section, as obtained by measuring the clean components under the same conditions The most significant changes of the Cr/Ni ratio were obtained when the electrode modified by 30 cycles was held for 2 min in the 0.5 M H_2SO_4 solution.

4. Discussion

Inconel-600 exhibits, an increase in voltammetric charge over a narrow potential range between 0.3 V and 0.4 V (under repetitive potential cycling conditions in 1 M NaOH solution, as seen in the Fig. 1). From literature data [11–13] it is known that this electrochemical process corresponds to a growth of a hydrous oxide film on the pure nickel electrode in an alkaline solution, due to $Ni(OH)_2$/NiOOH transition. Although Inconel-600 is a three-component Ni–Cr–Fe system, it is clear (Fig. 1) that the electrochemical process of the nickel component is predominant in the oxide growth. There is also a small peak at −1.0 V which occurs during the first scan in the positive direction, due to the Ni/$Ni(OH)_2$ transition. It was shown [27] that this peak might not appear beyond the first potential scan unless the potential was not held at −1.0 V for at least 1 min to reduce the $Ni(OH)_2$ component. The appearance of a small shoulder between 0.1 V and 0.3 V during the first potentiodynamic scan in the positive direction is, we believe, in agreement with the potentiodynamic profile of stainless steel [14] where a peak of chromium was detected in the same potential range, due to chromium oxidation. The iron component, which according to literature data for pure iron and stainless steel should appear at −1.0 V, is masked by the presence of $Ni(OH)_2$.

Electrochemical evidence for the formation of a hydrous oxide film under repetitive potential cycling conditions can be obtained by comparing the formation of the oxide film by two approaches, namely by repetitive potential cycling (Fig. 3(a)) and potentiostatic oxidation (Fig. 3(b)). As can be concluded from data presented in Fig. 3 and in Section 3.1, the repetitive potential cycling technique induces enhanced multilayer growth by more than one order of magnitude when compared to the potentiostatic method. Such growth results in the formation of a more open, hydrous and thicker oxide film. The main difference between the potentiostatic oxide growth and the oxide growth under potential cycling conditions is that, in the former case, the growth, as controlled by a place exchange mechanism [28], follows a direct or indirect logarithmic law [29]. The oxide growth under potential cycling conditions is controlled by a different mechanism. At a positive potential, the oxide grows in a usual way, that is, by place exchange, whereas at a negative potential the oxide is reduced.

Table 1 XPS data of Ni/Cr ratio of Inconel-600 electrodes

Sample	Cr/Ni as received*	Cr/Ni after sputtering†
1	0.41	0.59
2	0.56	0.44
3	0	0.07
4	1.60	1.32

* after electrochemical and chemical pretreatments (see Section 2).
† after sputtering for 1 min using Ar^+ at 300 eV.

The reduction process depends upon the metal studied and the experimental conditions carried out. After the reduction process metal atoms, which have already passed through several oxidation/reduction cycles, are in an 'activated' state [30] as induced by surrounding water and electrolyte molecules. Such a mixed layer of metal atoms and electrolyte and water molecules enable inclusion of additional, 'fresh', metal atoms in the oxidation process. In such a way, a porous and thick oxide film may be obtained. Certainly, during the film growth the place exchange is also an important process. However, it should be noted that in this case, the continuous oxidation and reduction processes lead to the formation of a duplex type of the oxide film, which consists of a compact inner oxide and an outer hydrous oxide film, as discussed by Burke and Lyons [1].

It is of interest to estimate the extent to which the Inconel-600 surface modification by formation of a hydrous oxide film influences its corrosion properties. As seen from Fig. 4, both the untreated and potentiodynamically treated electrodes exhibit a common E/log i behaviour with active, passive and transpassive ranges with identical E_{corr} values of −0.4 V. The current for the untreated electrode in both active and passive ranges is greater than that of the modified electrode. However, the identical E_{corr} values obtained for both the treated and untreated electrode indicate that, in both cases, the corrosion mechanism is the same though, as shown above, the reaction rates are different. In the case of the untreated electrode, the current in the active range is due to nickel and iron.

It is known that chromium species play a key role in the passive layer on stainless steels and nickel-based alloys [20]. The question is to what extent the modified layer is a protective barrier for oxidation of the bulk constituents of such an alloy. The answer is provided by RRDE measurements (Fig. 5) and the cyclic voltammogram in Fig. 7.

The ring current decrease indicates dissolution of the hydrous part of the oxide layer. At the comple-

tion of the dissolution process, it reaches the value of residual current of the electrochemically untreated electrode.

It is also known that the hydrous oxide film grown by repetitive potential cycling in alkaline solution on iron [12] and on iron and nickel in stainless steel [14] are not stable in acid solution. However, despite dissolution of nickel and iron in the present case, the overall stability of the modified Inconel-600 surface is increased.

The breakdown of the film is usually evidenced by a shift in corrosion potential of the metal surface towards negative potential values over the active range. Besides the anodic polarization plots (Fig. 4), the open-circuit potential measurements of the untreated Inconel-600 surface and that of the electrochemically modified electrode, showed different behaviour (Fig. 6).

The potential of the untreated electrode was, from the very beginning of the experiment at negative values. The potentiodynamically treated electrode exhibits different E/t behaviour: at the beginning it is at a positive value, which slowly decreases to 0.05 V. Beyond this value a sharp drop to −0.15 V is observed. This is similar to the case of pure nickel, when a Ni electrode in the passive state is brought to open circuit conditions [31]. In this case two pH-dependent arrests of potential (Flade potentials) are found [31] and can be explained as being a transition from a higher to a lower oxide state.

On the basis of the results obtained for Inconel-600 electrode by potentiodynamic treatment (Fig. 1), anodic polarization plots (Fig. 4), RRDE measurements (Fig. 5), open-circuit potential measurements (Fig. 6), cyclic voltammograms recorded after exposure of the grown oxide film to acid solution (Fig. 7) and X-ray photoelectron spectroscopy measurements (Table 1), we propose the following model for its enhanced stability. Potentiodynamic cycling enables deeper penetration into the bulk of the alloy and simultaneous formation of the hydrous oxide film in the same way as was the case with iron and nickel [8–13]. This process is more efficient as far as the increase of the film thickness and the charge storage capacity of the oxide film are concerned, in comparison with the potentiostatic oxidation of the electrode (Figs 3(a) and (b)).

During immersion in sulphuric acid a selective dissolution of nickel and iron takes place, as shown by RRDE measurements and supported by cyclic voltammograms (Fig. 7) recorded at point 2 of the open-circuit potential/time curve (Fig. 6) which shows the disappearance of the main voltammetric peaks of the $Ni(OH)_2/NiOOH$ transition.

The selective dissolution of nickel and iron results in the enrichment of chromium content in the surface and subsurface layers. Indeed, XPS measurements (Table 1) show a considerable enrichment of chromium content in the case of the cycled and in sulphuric acid treated electrode.

The percolation model of the passivity of stainless steels and Fe–Cr alloys, proposed by Newman and Sieradzki [32–34], can be partly adopted here. In their model, selective dissolution of iron creates clusters of –Cr–O–Cr– chains. In addition, the surface chromium atoms with two or more chromium atoms in their neighbourhood have a zero dissolution probability and thus contribute to enhanced stability. In our model of enhanced stability, repetitive potential cycling enables modification of the alloy structure by formation of a duplex oxide film. After selective dissolution of nickel and iron, more Cr_2O_3 clusters are available to form the protective layer. It should be pointed out that the protective layer does not consist only of Cr_2O_3 chains.

XPS measurements showed the enrichment of chromium relatively to nickel, but nickel atoms were also found in the surface and subsurface layers (Table 1). In a hydrous environment, as created by a repetitive potential cycling, metal oxide species might be additionally bridged together by hydrogen bonds. Indeed, these assumptions are in agreement with electrochemical and XPS measurements reported by Moffat and Latanision [35], who have found that in the passive state of chromium, hydrated chromium species are linked by water, hydroxide and oxide species.

5. Conclusions

The Inconel-600 electrode subjected to repetitive potential cycling in an alkaline solution exhibits an increase in voltammetric charge which can be attributed to the growth of a thick hydrous oxide film similar to the growth of a hydrous oxide film on pure nickel under similar experimental conditions. The hydrous oxide layer exhibits somewhat increased stability in sulphuric acid in comparison with the unmodified electrode.

This enhanced stability may be explained by a model which takes into account selective dissolution of nickel, and probably iron, as evidenced by the disappearance of the main $Ni(OH)_2/NiOOH$ voltammetric peak and supported by RRDE measurements. Consequently, an enrichment of chromium takes place, as shown by XPS measurements, contributing to an enhanced stability of the modified electrode in acid solution.

The proposed model is in agreement with the percolation model of passivity of stainless steels and Fe–Cr alloys [32–34].

Acknowledgements

This work was supported by the Ministry of Science and Technology of the Republic of Croatia (projects 1-07-162 and 1-03-056). The technical assistance of Momir Milunović and Srećko Karašić is gratefully acknowledged.

References

[1] L. D. Burke and M. E. G. Lyons, in 'Modern Aspects of Electrochemistry' (edited by R. E. White, J. O'M.

Bockris and B. E. Conway), No 18, Plenum Press, New York (1986), p. 169.
[2] E. J. M. O'Sullivan and E. J. Calvo, *in* 'Chemical Kinetics' (edited by R. G. Compton), Elsevier, Amsterdam (1987), p. 247.
[3] J. Mozota, M. Vuković and B. E. Conway, *J. Electroanal. Chem.* **114** (1980) 153.
[4] S. Gottesfeld and S. Srinivasan, *ibid.* **86** (1978) 89.
[5] L. D. Burke and E. J. M. O'Sullivan, *ibid.* **97** (1979) 123.
[6] L. D. Burke and T. A. M. Twomey, *ibid.* **167** (1984) 285.
[7] S. Trasatti, *in* 'Electrochemical Hydrogen Technologies' (edited by H. Wendt), Elsevier, Amsterdam (1990), p.1.
[8] L. D. Burke and D. P. Whelan, *J. Electroanal. Chem.* **109** (1980) 385.
[9] L. D. Burke and T. A. M. Twomey, *ibid.* **162** (1984) 101.
[10] A. Visintin, A. C. Chialvo, W. E. Triaca and A. J. Arvia, *ibid.* **225** (1987) 227.
[11] L. D. Burke and O. J. Murphy, *ibid.* **109** (1980) 379.
[12] L. D. Burke and M. E. G. Lyons, *ibid.* **198** (1986) 347.
[13] O. A. Albani, J. O. Zerbino, J. R. Vilche and A. J. Arvia, *Electrochim. Acta* **31** (1986) 1403.
[14] M. Vuković, *Corros. Sci.* **37** (1995) 111.
[15] B. MacDougall and M, J. Graham, *in* 'Corrosion Mechanism in Theory and Practice' (edited by P. Marcus and J. Oudar), Marcel Dekker, New York (1995), p. 143.
[16] A. J. Davenport and M. Sansone, *J. Electrochem. Soc.* **142** (1995) 725.
[17] W. E. O'Grady and J. O'M. Bockris, *Surf. Sci.* **38** (1973) 249.
[18] R. W. Revie, B. G. Baker and J. O'M. Bockris, *J. Electrochem. Soc.* **122** (1975) 1460.
[19] W. E. O'Grady, *ibid.* **127** (1980) 555.
[20] G. Okamoto, *Corros. Sci.* **13** (1973) 471.
[21] H. H. Uhlig,'Corrosion and Corrosion Control', J. Wiley, New York (1963).
[22] Proceedings of the Symposium on Corrosion Protection by Coatings and Surface Modification (edited by M. W. Kendig, K. Sugimoto and N. R. Sorensen), The Electrochemical Society, Pennington, NJ (1993).
[23] L. Kwiatkowski and F. Mansfeld, *J. Electrochem. Soc.* **140** (1993) L39.
[24] S. B. Lalvani and G. Zhang, *Corros. Sci.* **37** (1995) 1583.
[25] M. Vuković, *J. Chem. Soc. Faraday Trans.* **86** (1990) 3743.
[26] D. Marijan and M. Vuković, unpublished results .
[27] M. Vuković, *J. Appl. Electrochem.* **24** (1994) 878.
[28] N. Sato and M. Cohen, *J. Electrochem. Soc.* **111** (1964) 512.
[29] B. E. Conway, B. Barnett, H. Angerstein-Kozlowska and B. V. Tilak, *J. Chem. Phys.* **93** (1990) 8361.
[30] L. D. Burke, J. J. Borodzinski and K. J. O'Dwyer, *Electrochim. Acta* **35** (1990) 967.
[31] N. Sato and G. Okamoto, *in* 'Comprehensive Treatise of Electrochemistry', Vol. 4, (edited by J. O'M. Bockris, B. E. Conway, E. Yeager and R. E. White), Plenum Press, New York (1981), p. 193.
[32] K. Sieradzki and R. C. Newman, *J. Electrochem. Soc.* **133** (1986) 1979.
[33] R. C. Newman, Fooung Tuck Meng and K. Sieradzki, *Corros. Sci.* **28** (1988) 523.
[34] S. Quian, R. C. Newman, R. A. Cottis and K. Sieradzki, *J. Electrochem. Soc.* **137** (1990) 435.
[35] T. P. Moffat and R. M. Latanision, *ibid.* **139** (1992) 1869.